PHYSICAL REVIEW E **89**, 010701(R) (2014)

Bifurcation in epigenetics: Implications in development, proliferation, and diseases

Daniel Jost

Laboratoire de Physique, École Normale Supérieure de Lyon, CNRS UMR 5672, Lyon, France

(Received 20 August 2013; revised manuscript received 14 November 2013; published 23 January 2014)

Cells often exhibit different and stable phenotypes from the same DNA sequence. Robustness and plasticity of such cellular states are controlled by diverse transcriptional and epigenetic mechanisms, among them the modification of biochemical marks on chromatin. Here, we develop a stochastic model that describes the dynamics of epigenetic marks along a given DNA region. Through mathematical analysis, we show the emergence of bistable and persistent epigenetic states from the cooperative recruitment of modifying enzymes. We also find that the dynamical system exhibits a critical point and displays, in the presence of asymmetries in recruitment, a bifurcation diagram with hysteresis. These results have deep implications for our understanding of epigenetic regulation. In particular, our study allows one to reconcile within the same formalism the robust maintenance of epigenetic identity observed in differentiated cells, the epigenetic plasticity of pluripotent cells during differentiation, and the effects of epigenetic misregulation in diseases. Moreover, it suggests a possible mechanism for developmental transitions where the system is shifted close to the critical point to benefit from high susceptibility to developmental cues.

DOI: 10.1103/PhysRevE.89.010701 PACS number(s): 87.18.Vf, 05.10.−a, 05.45.−a, 87.17.Aa

Cellular differentiation occurs during the development of multicellular organisms and leads to the formation of many different tissues where gene expression is modulated without modification of the genetic information [1]. These modulations are in part encoded by biochemical tags, called epigenetic marks, that are set down at the chromatin level directly on DNA or on histone tails. These marks are directly or indirectly involved in the local organization and structure of the chromatin fiber, and therefore may modulate the accessibility of DNA to transcription factors or enzymatic complexes, playing a fundamental role in the transcriptional regulation of gene expression.

Each tissue is characterized by a distinct epigenetic pattern [2] that is mainly shaped during cellular differentiation by developmental signals driven mainly by transcription factors. For a differentiated cell, these specific signals disappear and the global epigenetic state of a cell is robustly maintained throughout the cell life and in its daughter cells. This maintenance, despite the fast turnover rate of epigenetic marks [3] or the dilution of epigenetic information during cell division [4], implies the existence of mechanisms to avoid the rapid loss of epigenetic information.

At the gene level, there are active or inactive epigenetic marks that influence the transcriptional activity of the gene [5]. A coherent activity needs the gene promoter to be covered by a majority of active or inactive marks. Recently, many efforts both experimentally [6–8] and theoretically [9–18] have been dedicated to study the mechanisms responsible for the spreading and maintenance of an epigenetic state at the gene level for different biological organisms and contexts. In particular, it has been shown for many examples, such as for the locus *MAT* in fission yeast [9,12] or for the vernalization of the floral repressor *FLC* in *Arabidopsis* [7,15], that long-range or cooperative interactions between epigenetic marks are necessary for the emergence of stable coherent states. Of particular interest is also the work of the Sengupta group, showing that differences between activating and silencing rates might be responsible for hysteresis in epigenetic silencing by the silent information regulator (SIR) system in budding yeast [11,18].

In this Rapid Communication, we develop a general formalism that describes the dynamics of epigenetic marks and that accounts, at the same time, for the plasticity and robustness of the epigenome. Using statistical and nonlinear physics methods, we characterize the emergence of coherent epigenetic states from the recruitment of modifying enzymes and we study the bifurcations occurring in the system when altering the recruitment intensities. Finally, we discuss in detail the implications of our findings in concrete biological contexts during development, differentiation, or disease. In particular, we propose that the experimentally observed regulation of the cell cycle during development might have a strong impact on the efficiency of epigenetic switches.

a. Model. Inspired by the model introduced by Dodd *et al.* for the mating-type switch of the fission yeast (*S. pombe*) [9,10,12], we consider a DNA region, consisting of n nucleosomes, that is located between two boundaries that epigenetically isolate the region from neighboring DNA [13,19]. We assume that the epigenetic state of each nucleosome can fluctuate between three different states: unmarked (U), active (A), and inactive (I). Active marks would be, for example, associated with acetylation of the lysine 9 of histone 3 (H3K9), and inactive marks with tri-methylation of H3K9 (HP1-type chromatin) or with the methylation of H3K27 (Polycomb-type chromatin) [5]. However, the actual epigenetic marks associated with each state are not important for our purpose and we only need two well-separated kinds of marks that can be exchanged to each other by passing through an intermediate state ($I \rightleftharpoons U \rightleftharpoons A$).

We assume that the nucleosomal state can be modified by two mechanisms: (i) Recruitment of modifying enzymes (for example, histone demethyl- or methyltransferases and histone deacetyl- or acetyltransferases) by surrounding active or inactive nucleosomes that occurs at a rate $\epsilon_X \rho_X$ where ρ_X is the local density of the modified state X (A or I) that, by considering a spatial mean-field approximation, we identified to the *global* density n_X/n with n_X the corresponding number of nucleosomes. (ii) Random transitions between states that occur at a rate k_0 and that represents recruitment-independent

enzymatic activity, nucleosome turnover, or dilution due to replication. Note that to facilitate the analysis, we lumped into k_0 processes (turnover vs replication) with presumably different time scales and statistical properties. However, previous works on epigenetic modeling [9,10] suggest that the main conclusions of our study should not depend on that approximation. The corresponding system of biochemical reactions is composed of four possible state transitions given below with their respective propensities:

$$U \to A, \quad r_{u,a} \equiv (k_0 + \epsilon_A \rho_A)(n - n_A - n_I), \tag{1}$$

$$U \to I, \quad r_{u,i} \equiv (k_0 + \epsilon_I \rho_I)(n - n_A - n_I), \tag{2}$$

$$A \to U, \quad r_{a,u} \equiv (k_0 + \epsilon_I \rho_I) n_A, \tag{3}$$

$$I \to U, \quad r_{i,u} \equiv (k_0 + \epsilon_A \rho_A) n_I, \tag{4}$$

where, for simplicity, we assumed that the rates of random transitions are similar for each reaction and that possible discrepancies between A and I occur at the recruitment level.

b. Analogy with an Ising model and phase transitions. From a theoretical perspective, we remark that this model is formally very similar to a zero-dimensional three-state Ising model where nucleosomal states represent spins (for example, $I = -1$, $U = 0$, $A = +1$), recruitment (ϵ_X) corresponds to coupling between spins (J), and random transitions (k_0) are associated with thermal fluctuations ($k_B T$).

This analogy suggests that a good observable for our system will be the magnetization $m = (n_A - n_I)/n$. In biological terms, this magnetization could be interpreted as the relative activity of the DNA region if we consider that, in addition to the favorable effect of active marks, the presence of inactive marks penalizes the activity. In the following, we will consider m as the relevant observable of our system.

As it is well known that zero-dimensional Ising models do exhibit phase transitions between ordered and disordered phases [20], we expect our system to display such dramatic changes. To illustrate this, we consider the simple mass-action model (equivalent to the mean-field approximation of the Ising model) that captures the mean dynamics of the epigenetic marks in the case of symmetric recruitment ($\epsilon_A = \epsilon_I \equiv \epsilon$):

$$\frac{d\rho_A}{dt} = (k_0 + \epsilon\rho_A)(1 - \rho_A - \rho_I) - (k_0 + \epsilon\rho_I)\rho_A, \tag{5}$$

$$\frac{d\rho_I}{dt} = (k_0 + \epsilon\rho_I)(1 - \rho_A - \rho_I) - (k_0 + \epsilon\rho_A)\rho_I. \tag{6}$$

At the steady state, the previous dynamical system has, at most, three relevant fixed points that, in term of the effective magnetization m, are given by $m_0 = 0$ ($\forall\epsilon$) and $m_\pm = \pm(k_0/\epsilon)\sqrt{(\epsilon/k_0 + 1)(\epsilon/k_0 - 3)}$ (for $\epsilon > 3k_0$). Figure 1(a) shows the classical supercritical pitchfork bifurcation occurring at the critical point $\epsilon_c = 3k_0$. For weak recruitment ($\epsilon < \epsilon_c$), m_0 is the only stable fixed point and the activity of the DNA region is not clearly defined. At the critical point, m_0 turns unstable and stable coherent activities ($m_\pm$ for active or inactive) are only observed for strong recruitments ($\epsilon > \epsilon_c$).

c. Distribution and stability of epigenetic states. To go beyond the mean-field approximation, we aim at the full distribution of probability for m. For simplicity, we assume symmetric coupling in the following. The general situation

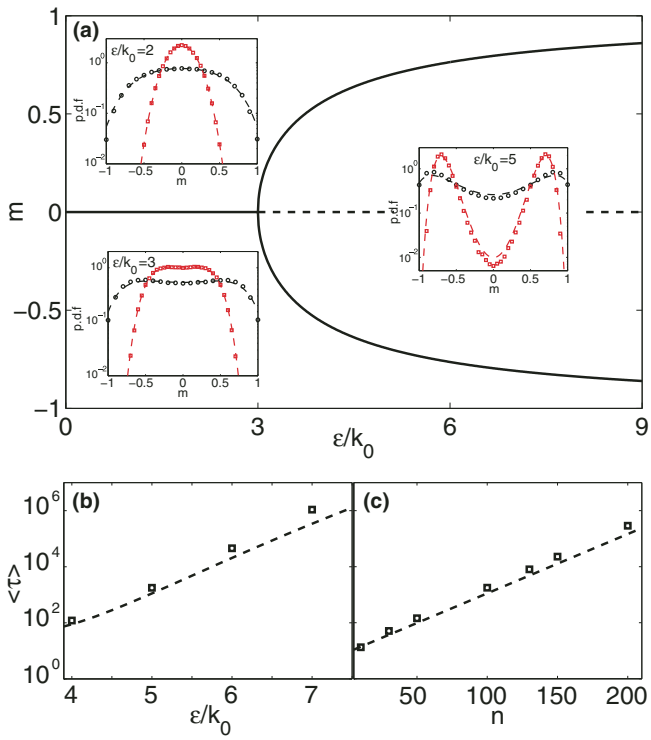

FIG. 1. (Color online) Symmetric regime. (a) Bifurcation diagram for m as a function of ϵ/k_0. Full (dashed) lines represent stable (unstable) fixed points of the dynamical system. Insets: Probability distribution functions (p.d.f.) of m for $n = 10$ (black circles) or $n = 100$ (red squares) computed from the Fokker-Planck approximation (dashed lines) or from stochastic simulations (squares). (b),(c) Mean first passage time $\langle\tau\rangle$ (in k_0^{-1} units) to switch from m_- to m_+ as a function of ϵ [(b) for $n = 100$] or of n [(c) for $\epsilon/k_0 = 5$], computed from Eq. (9) (dashed lines) or from simulations (squares). Standard errors on the estimation of $\langle\tau\rangle$ are smaller than the symbol size.

will be discussed in the next section. The starting point is to write the master equation related to the set of biochemical reactions given in Eqs. (1)–(4), but for the variables m and $s = (n_A + n_I)/n$ where s represents the density of marked nucleosomes. Then, assuming that s is always large and that its dynamics is fast compared to the one of m allows one to perform a time-scale separation and leads, in the limit of large n, to the Fokker-Planck equation for the probability $P(m)$ (see Supplemental Material [21] for details),

$$\frac{\partial P}{\partial t} = -\frac{\partial}{\partial m}\Big([w_+(m) - w_-(m)]P - (1/2n)\frac{\partial}{\partial m}\{[w_+(m) + w_-(m)]P\}\Big), \tag{7}$$

with $w_+ = (r_{u,a} + r_{i,u})/n$ and $w_- = (r_{u,i} + r_{a,u})/n$, the propensities to increase (using reactions 1 and 4) or decrease (2 and 3) m by 1. Equation (7) is a classical Fokker-Planck equation for the heterogeneous diffusion of a particle within a unidimensional potential [22,23]. At the steady state, the probability distribution is then given by

$$P_\infty(m) = \frac{1}{Z}\frac{\exp\left\{2n\int_{-\infty}^{m} dm' \left[\frac{w_+(m') - w_-(m')}{w_+(m') + w_-(m')}\right]\right\}}{w_+(m) + w_-(m)}, \tag{8}$$

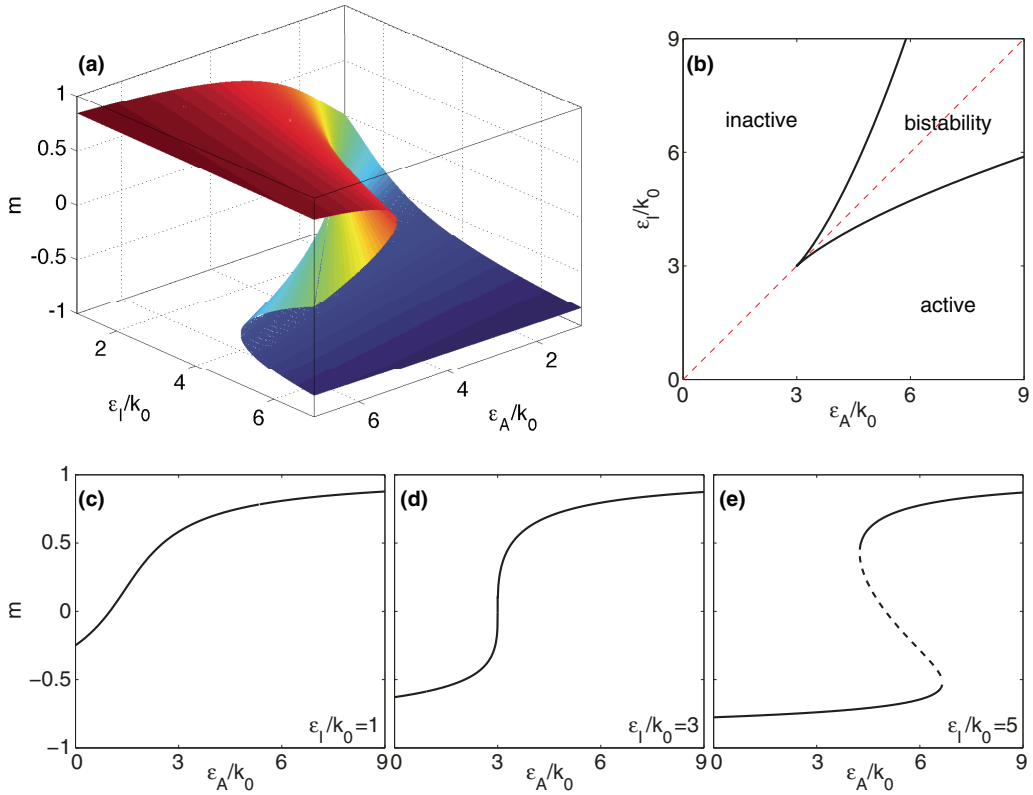

FIG. 2. (Color online) Asymmetric regime. (a) Cusp catastrophe surface representing the fixed points of the dynamical system as a function of ϵ_A/k_0 and ϵ_I/k_0. (b) Stability diagram and boundaries between the mono- and bistable regions. (c)–(e) Bifurcation diagrams for m as a function of ϵ_A/k_0 for fixed values of ϵ_I/k_0 [(c) = 1, (d) = 3, (e) = 5]. Legend as in Fig. 1(a).

with Z a normalization factor. The insets of Fig. 1(a) show the very good agreement between the approximated solutions given by Eq. (7) and the distributions computed from exact stochastic simulations of the full system (1)–(4) using the Gillespie algorithm [24]. While below the critical point we observe a unimodal distribution centered around m_0, for high coupling ($\epsilon > \epsilon_c$), the distribution is bimodal and peaked around the coherent epigenetic states $m_\pm$, with the width of each peak being proportional to $[n(\epsilon - \epsilon_c)/k_0]^{-1/2}$ [21]. At the critical point, we observe a nearly flat distribution, characteristic of phase transitions.

In the presence of bimodality, we quantify the stability of a coherent epigenetic state by computing the mean first passage time $\langle\tau\rangle$ to switch from m_- to m_+. Using the Fokker-Planck formalism introduced above, we show that [21]

$$\langle\tau\rangle \approx \frac{18\pi}{(\epsilon - \epsilon_c)\sqrt{3(\epsilon/k_0 + 3)}} \exp[V(0) - V(m_-)], \qquad (9)$$

with $V(m) = -\log P_\infty$ the effective potential corresponding to the steady-state "epigenetic landscape." As already pointed out by Micheelsen *et al.* [12], we find that similar to transition state theory [25], $\langle\tau\rangle$ mainly depends on the "energy barrier" between the starting state ($m = m_-$) and the transition state ($m = 0$). As the coupling increases, the barrier is higher and the epigenetic state is more stable [see Fig. 1(b)]. We also remark that $\langle\tau\rangle$ scales exponentially with the size n of the system [see Fig. 1(c)]. Such very long relaxation times are typical to systems with long-range interactions [20,26] and means that the larger the system, the more stable the epigenetic state.

d. Asymmetry and cusp catastrophe. In this section, we consider the general situation where recruitments of enzymes by active or inactive marks are different. In the next section, we will focus on the study of the generalization of the dynamical system, given by Eqs. (5) and (6), which captures the main characteristics of asymmetric recruitment.

At the steady state, the system has, at most, three fixed points and the bifurcation diagram shapes as a cusp catastrophe surface [Fig. 2(a)], which is characteristic of dynamical systems with asymmetry [27] and also observed, for example, in the epigenetic SIR system in budding yeast [11,18] or in insect outbreaks [28]. For every pair of parameters (ϵ_A,ϵ_I), the dynamical system is either monostable or bistable (with an unstable fixed point). Using equality conditions on the nullclines and their first derivatives [21], we find an exact parametric expression for the boundary between the mono- and bistable regions [Fig. 2(b)]. Depending on the relative asymmetry between ϵ_A and ϵ_I, the single (stable) fixed point of the monostable region corresponds to an active or inactive epigenetic state. Bistability, with the coexistence of an active and an inactive coherent activity, is observed only for strong recruitments (ϵ_A,$\epsilon_I > \epsilon_c$) and small asymmetry.

Figures 2(c)–2(e) show the bifurcation diagram of the system when increasing ϵ_A/k_0 for fixed values of ϵ_I/k_0. If $\epsilon_I < \epsilon_c$, the system stays in the monostable region and the unique fixed point goes continuously from an almost incoherent state ($m \sim 0$) to a coherent active state [Fig. 2(c)]. For stronger recruitment ($\epsilon_I > \epsilon_c$), the system crosses the bistable region making a typical hysteresis curve with two saddle-node

bifurcations [Fig. 2(e)]. For example, starting from an inactive state, as we increase the recruitment of active marks, the system stays in the inactive state (even for $\epsilon_A > \epsilon_I$) until it switches abruptly to an active state. When crossing the cusp point [Fig. 2(d)], the system becomes ultrasensitive and weak asymmetries lead to important changes in the epigenetic state.

e. Implications in development, proliferation, and diseases. Recent quantitative experiments in mice [8] have shown that bistable activities take place in an epigenetically controlled system and that modifications in the epigenome can be stably imprinted by transcriptional factors. In particular, this study suggests that, at least for some chromatin regions, symmetric or weakly asymmetric recruitment may correspond to normal biological situations, and that temporary strong asymmetries in the recruitment of modifying enzymes may lead to long-term modifications of the current epigenetic state.

In vivo, differentiated cells exhibit a robust phenotype within the population and in time. The analysis of the symmetric regime of our formalism (Fig. 1) suggests that such robustness needs strong recruitments ($\epsilon > \epsilon_c$) and large cooperative units ($n \gg 1$) in order to stabilize coherent epigenetic states (active or inactive) and to avoid spurious switches between coherent states. Moreover, Fig. 2 suggests that epigenetic states of differentiated cells are also stable against small fluctuations of the recruitment couplings. Such fluctuations induce asymmetries in the system that do not impact significantly on the epigenetic state as long as ϵ_A and ϵ_I remain in the bistability region. This property is crucial for the maintenance of a robust phenotype in weakly fluctuating environments.

However, when modifications of the environment are important, it would be beneficial to adapt to the current environment by modifying the epigenetic state, such as, for example, for plants at seasonal transitions [29]. Misadaptation to the current environment may lead to stress signalings that might result in asymmetric recruitment forcing the current epigenetic state towards an adapted state, such as in the cold-induced silencing of the *FLC* locus in plant vernalization [7]. Figure 2(e) suggests that such asymmetric signals have to be strong enough to allow an epigenetic switch. Once the switch is performed, the hysteretic shape of the bifurcation insures that the epigenome will remain stable in its new state. This property allows adaptation but only if needed, i.e., only when the organism is strongly misadapted to the current environment.

Many diseases have been related to epigenetic perturbations, from neurologic disorder to cancer [30]. Within our formalism, these perturbations could be interpreted by anomalous values for the recruitment (ϵ/k_0) that shift the steady state of the system below or close to the critical point, and that make the epigenetic state incoherent or unstable and very sensitive to external noise. For example, cancer is often associated with an increase in the frequency of replication during tumorigenesis [31]. In our model, this means an increase of the random transition rate k_0 due to replication. This may modify the position of the critical point and therefore may lead to epigenetic instability and misregulation of some tumor suppressor proteins, for example.

During development, cellular differentiation occurs in successive stages. Cells pass through a series of developmental transitions where epigenetic states are modified by developmental cues that presumably force locally the desired state. Previously, we saw that, for differentiated cells, the hysteretic shape of the bifurcation may be valuable for the buffering of environmental fluctuations or for adaptation. Within the context of development, this could represent a hindrance at developmental transitions when the epigenetic state has to efficiently switch in a short time window. Our formalism suggests that a possible strategy to overcome this apparent issue would be to temporarily shift the system at or close to the critical point during developmental transition. Indeed, Fig. 2(d) shows that at the cusp point, the epigenetic state is very sensitive to weak asymmetries. Going back to the original analogy between our model and an Ising model with

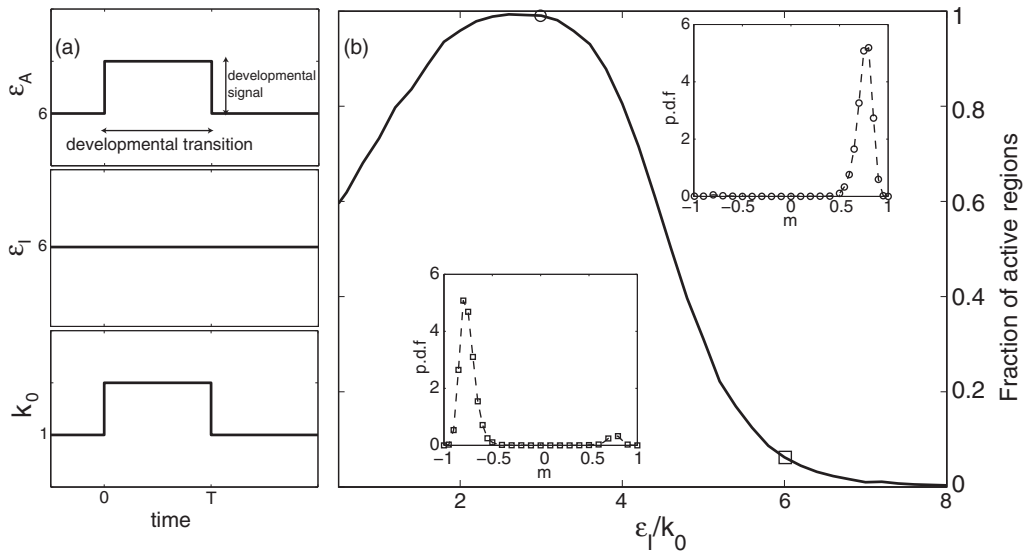

FIG. 3. Epigenetics and criticality. (a) Proposed strategy for guided epigenetic switching at developmental transitions when temporary asymmetric signal ($\epsilon_A > \epsilon_I = 6$) and modification of k_0 are applied during a finite time period T. (b) Probability to be active ($m > 0$) after a time $t = 100$ starting from a silenced state ($m = m_-$) as a function of the effective recruitment strength ϵ_I/k_0 for $\epsilon_A = 8$ and $T = 5$. Insets: Corresponding probability distribution function of m at $\epsilon_I/k_0 = 3$ (circles) or 6 (squares).

phase transition, this is related to the concept of susceptibility that is maximal at the critical point. In many organisms, experimental evidence suggests that the cell cycle length is regulated during development, alternating between short cycles during developmental transitions and longer cycles between the transitions and in the differentiated state [32]. In our model, this means that at developmental transitions, k_0 may be increased and therefore the effective recruitment strength (ϵ/k_0) may be reduced and may become closer to the critical value. Under this hypothesis, we test the ability to switch between two coherent states when applying a weak asymmetric signal (the developmental signal) during a finite time period (the developmental transition) by running Gillespie simulations. As expected, Fig. 3 shows that the switching efficiency is optimal when $\epsilon_I/k_0 \sim 3$ during the transition. Compared to the situation where k_0 is not changed during the transition and where only a few cells have switched their epigenetic state, going close to the critical point leads to a stable switch for almost all of the cells. Assuming the necessary experimental verifications of the proposed strategy, our results strongly suggest that it could be advantageous, during developmental transitions, to be close to criticality to benefit from the high sensitivity to external stimuli, as already observed in various other biological systems [33].

I thank Cédric Vaillant for fruitful discussions.

[1] C. D. Allis, T. Jenuwein, and D. Reinberg, *Epigenetics* (Cold Spring Harbor Laboratory Press, New York, 2007).
[2] A. Doi, I.-H. Park, B. Wen, P. Murakami, M. J. Aryee, R. Irizarry, B. Herb, C. Ladd-Acosta, J. Rho, S. Loewer, J. Miller, T. Schlaeger, G. Q. Daley, and A. P. Feinberg, Nat. Genet. **41**, 1350 (2009).
[3] R. B. Deal, J. G. Henikoff, and S. Henikoff, Science **328**, 1161 (2010).
[4] R. Margueron, and D. Reinberg, Nat. Rev. Genet. **11**, 285 (2010).
[5] T. Jenuwein, and C. D. Allis, Science **293**, 1074 (2001).
[6] J. Z. Kelemen, P. Ratna, S. Scherrer, and A. Becksei, PLoS Biol. **8**, e1000332 (2010).
[7] A. Angel, J. Song, C. Dean, and M. Howard, Nature (London) **476**, 105 (2011).
[8] N. A. Hathaway, O. Bell, C. Hodges, E. L. Miller, D. S. Neel, and G. R. Crabtree, Cell **149**, 1447 (2012).
[9] I. A. Dodd, M. A. Micheelsen, K. Sneppen, and G. Thonn, Cell **129**, 813 (2007).
[10] D. David-Rus, S. Mukhopadhyay, J. L. Lebowitz, and A. M. Sengupta, J. Theor. Biol. **258**, 112 (2009).
[11] S. Mukhopadhyay, V. H. Nagaraj, and A. M. Sengupta, BioSystems **102**, 49 (2010).
[12] M. M. Micheelsen, N. Mitarai, K. Sneppen, and I. B. Dodd, Phys. Biol. **7**, 026010 (2010).
[13] I. B. Dodd and K. Sneppen, J. Mol. Biol. **414**, 624 (2011).
[14] A. Becksei, S. Scherrer, J. Z. Kelemen, and A. E. Murray, Transcription **2**, 173 (2011).
[15] A. Satake and Y. Iwasa, J. Theor. Biol. **302**, 6 (2012).
[16] K. Sneppen, and I. B. Dodd, PLoS Comp. Biol. **8**, e1002643 (2012).
[17] H. Binder, L. Steiner, J. Przybilla, T. Rohlf, S. Prohaska, and J. Galle, Phys. Biol. **10**, 026006 (2013).
[18] A. Dayarian, and A. M. Sengupta, Phys. Biol. **10**, 036005 (2013).
[19] M. Gaszner and G. Felsenfeld, Nat. Rev. Genet. **7**, 703 (2006).
[20] D. Mukamel, S. Ruffo, and N. Schreiber, Phys. Rev. Lett. **95**, 240604 (2005).
[21] See Supplemental Material at http://link.aps.org/supplemental/10.1103/PhysRevE.89.010701 for details of the derivations of the Fokker-Planck equation and of the bifurcation diagrams.
[22] N. van Kampen, *Stochastic Processes in Physics and Chemistry* (North-Holland, Amsterdam, 2001).
[23] H. Risken, *The Fokker-Planck Equation* (Springer-Verlag, Berlin, 1989).
[24] D. T. Gillespie, J. Phys. Chem. **81**, 2340 (1977).
[25] K. J. Laidler, *Theories of Chemical Reaction Rates* (McGraw-Hill, New York, 1969).
[26] F. Bouchet, Physica A **389**, 4389 (2010).
[27] S. H. Strogatz, *Nonlinear Dynamics and Chaos* (Westview, Boulder, CO, 1994).
[28] D. Ludwig, D. D. Jones, and C. S. Holling, J. Anim. Ecol. **47**, 315 (1978).
[29] D. Horvath, Plant Sci. **177**, 523 (2009).
[30] A. Portela and M. Esteller, Nat. Biotechnol. **28**, 1057 (2010).
[31] M. Malumbres and M. Barbacid, Nat. Rev. Cancer **9**, 153 (2009).
[32] Y. Budirahardja and P. Gonczy, Development **136**, 2861 (2009).
[33] T. Mora and W. Bialek, J. Stat. Phys. **144**, 268 (2011).